BNL–HET–00/18
hep-ph/0006280

Direct CP violation in radiative b decays in and beyond the Standard Model

Ken Kiers[a*], Amarjit Soni[b†] and Guo-Hong Wu[c‡]

[a] *Physics Department, Taylor University*
236 West Reade Ave., Upland, IN 46989

[b] *High Energy Theory, Department of Physics*
Brookhaven National Laboratory,Upton, NY 11973-5000

[c] *Institute of Theoretical Science, University of Oregon, Eugene, OR 97403-5203*

Abstract

We consider the partial rate asymmetry in the inclusive decay modes $b \to s\gamma$ and $b \to d\gamma$, concentrating on non-standard models with new charged Higgs interactions. We find that the charged Higgs contribution to the asymmetry for $b \to s\gamma$ is small in such models due to a universal cancellation mechanism. The asymmetry is therefore difficult to distinguish experimentally from the Standard Model (SM) value, which is also small. The cancellation mechanism is found to be rendered inoperative in supersymmetry due to the presence of chargino loops. Unlike $b \to s\gamma$, the rate asymmetry for $b \to d\gamma$ in Higgs models can be quite different from its SM value, generally ranging from -20% to $+20\%$. Specific model calculations are performed for the Three-Higgs Doublet Model and the "Top" Two-Higgs Doublet Model to serve as illustrations. We also offer some suggestions that may be helpful to experimentalists in the detection of the inclusive mode $b \to d\gamma$.

PACS numbers: 11.30.Er, 12.60.Fr, 13.25.Hw, 14.80.Cp

*Email: knkiers@tayloru.edu, †soni@bnl.gov, ‡wu@dirac.uoregon.edu

I. INTRODUCTION

The e^+e^--based B-factories are all performing quite well. Each of them should soon be producing of order 10^7 B-$\overline{B}$ pairs per year in a very clean environment. In another few years it is likely that one or more of these machines will yield of order 10^8 B-$\overline{B}$ pairs per year. B-experiments at the hadron machines – Tevatron (BTEV), Hera-B and LHC-B – could increase this number by another 1-3 orders of magnitude. Therefore, studies of rare B-decays will continue to intensify for the next several years.

Radiative B decays have been the subject of much theoretical and experimental interest over the past several years. While $b \to s\gamma$ is loop-suppressed within the SM, it nevertheless has a relatively large branching ratio, allowing for a very important comparison between theory and experiment. A recent measurement of the branching ratio by CLEO [1] yielded the value $\mathcal{B}(b \to s\gamma) = (3.15 \pm 0.35 \pm 0.32 \pm 0.26) \times 10^{-4}$, in good agreement with the ALEPH measurement [2] and the SM prediction [3–5]. The good agreement between the experimental and theoretical branching ratios places a strong constraint on many non-standard models. The recent CLEO measurements [1] have also placed a rather modest bound on the partial rate asymmetry (PRA) in $b \to s\gamma$, yielding $-9\% < A_{CP}^{b\to s\gamma} < 42\%$ at the 90% confidence level. This bound does not yet encroach on the very small PRA (of order 0.6%) predicted by the SM [6]. Improved measurements of $A_{CP}^{b\to s\gamma}$ are expected over the next several years at the B-factories. These measurements should provide a powerful probe of new physics, particularly of models that contain non-standard CP-odd phases.

A mode closely related to $b \to s\gamma$ that is also of great interest is $b \to d\gamma$. The branching fraction for this mode is expected to be of order 10^{-5}, so a good measurement of the branching fraction should be possible with the 10^8 B-$\overline{B}$ pairs per year expected at the B-factories, provided the difficulties in the experimental detection of $b \to d\gamma$ can be overcome (see below). The PRA for $b \to d\gamma$ is of order -16% within the SM and may also be observable within the next several years. It is important to note that the SM PRA for $b \to d\gamma$ is *statistically* more accessible than that for $b \to s\gamma$. That is, the increase in the PRA for $b \to d\gamma$ relative to that for $b \to s\gamma$ more than compensates the suppression of its branching ratio. This statement is relatively robust and holds true even after making reasonable concessions for detection efficiencies in the two cases, as we discuss in Sec. V C. The statistical accessibility of $A_{CP}^{b\to d\gamma}$ is quite intriguing and leads us to a serious consideration of this observable in the present paper. A discussion of some practical experimental techniques for distinguishing $b \to d\gamma$ from $b \to s\gamma$ may be found in Sec. V.

Our goal in the present work is to assess the sensitivity of the rate asymmetries noted above to effects coming from various non-standard models. Our main emphasis is on effects due to the exchange of charged Higgs bosons, but we offer insights regarding other models as well. A summary of our main results as well as those of some previous authors may be found in Table I. Previous studies of the $b \to s\gamma$ PRA due to charged Higgs exchange have generically found quite small values [7–10]. In this paper we will show that this trend is due to a partial cancellation between terms in a general expression for the rate asymmetry. The cancellation is a nearly universal feature of models containing only new charged Higgs interactions, and typically constrains $b \to s\gamma$ rate asymmetries in such models to be at or below the few-percent level. Experimentally, such values would be difficult to distinguish from the (similarly small) value expected within the SM. A contrasting situation is found

for $b \to d\gamma$ [8]. In this case the PRA can differ appreciably from the SM result, in general ranging between -20% and $+20\%$.

The outline of the remainder of the paper is as follows. In Sec. II we review the general formalism used to calculate the PRA for inclusive radiative b decays. In Sec. III we focus specifically on Higgs models and show that $A_{CP}^{b\to s\gamma}$ is destined to be quite small in such models, while $A_{CP}^{b\to d\gamma}$ can be both large and different from its SM value. These general features are illustrated by calculations in a few specific Higgs models, namely in the Three-Higgs Doublet Model (3HDM) with Natural Flavour Conservation and the Top-Two-Higgs Doublet Model (T2HDM). Section IV contains a general discussion of supersymmetric effects on the asymmetries and shows how supersymmetric models manage to evade the accidental cancellation that Higgs models face. Section V contains a discussion of some practical experimental techniques that could be useful in distinguishing between $b \to d\gamma$ and $b \to s\gamma$. In Sec. VI we offer a few concluding remarks, as well as a summary of our results.

II. GENERAL FORMALISM

Let us begin by reviewing the general formalism used to calculate the PRA in inclusive radiative B decays. Further details of the calculation may be found in Ref. [9]. The PRA in the inclusive decay $b \to s\gamma$ is defined by the ratio

$$A_{CP}^{b\to s\gamma} = \frac{\Gamma(\overline{B} \to X_s\gamma) - \Gamma(B \to X_{\overline{s}}\gamma)}{\Gamma(\overline{B} \to X_s\gamma) + \Gamma(B \to X_{\overline{s}}\gamma)} \,. \tag{1}$$

The next-to-leading order expression for the asymmetry may be found in Ref. [9] and is expressed in terms of the Wilson coefficients C_i as

$$A_{CP}^{b\to s\gamma} = \frac{\alpha_s(m_b)}{|C_7|^2} \left\{ \frac{40}{81} \mathrm{Im}\left[C_2 C_7^*\right] - \frac{8z}{9}\left[v(z) + b(z,\delta_\gamma)\right] \mathrm{Im}\left[(1+\epsilon_s) C_2 C_7^*\right] \right.$$
$$\left. - \frac{4}{9} \mathrm{Im}\left[C_8 C_7^*\right] + \frac{8z}{27} b(z,\delta_\gamma) \mathrm{Im}\left[(1+\epsilon_s) C_2 C_8^*\right] \right\}, \tag{2}$$

where $z = m_c^2/m_b^2 \simeq (0.29)^2$ and

$$\epsilon_s = \frac{V_{us}^* V_{ub}}{V_{ts}^* V_{tb}} \simeq -\lambda^2(\rho - i\eta). \tag{3}$$

The second term in Eq. (3) gives an approximation to ϵ_s, written in the usual Wolfenstein parameterization, with $\lambda \simeq 0.22$. The functions $v(z)$ and $b(z,\delta_\gamma)$ are defined in Ref. [9]; δ_γ is related to the experimental cut on the photon energy: $E_\gamma > (1-\delta_\gamma)E_\gamma^{\max}$. An analogous CP asymmetry can be constructed for the decay $b \to d\gamma$ and gives an expression similar to Eq. (2), but with the replacement $\epsilon_s \to \epsilon_d$, where [9]

$$\epsilon_d = \frac{V_{ud}^* V_{ub}}{V_{td}^* V_{tb}} \simeq \frac{\rho - i\eta}{1 - \rho + i\eta}. \tag{4}$$

Kagan and Neubert have evaluated the coefficients of the various terms in Eq. (2) for different values of the photon energy cut-off, δ_γ. They have also performed a more elaborate

calculation to take into account the effects of Fermi motion [9]. For our purposes it is sufficient to neglect the Fermi-motion effects and to choose a particular value of δ_γ. Choosing $\delta_\gamma = 0.30$, and taking $\alpha_s(m_b) \simeq 0.214$, we find

$$A_{CP}^{b\to s(d)\gamma} \simeq \frac{10^{-2}}{|C_7|^2}\Big\{1.17 \times \mathrm{Im}\left[C_2 C_7^*\right] - 9.51 \times \mathrm{Im}\left[C_8 C_7^*\right] + 0.12 \times \mathrm{Im}\left[C_2 C_8^*\right] \\ -9.40 \times \mathrm{Im}\left[\epsilon_{s(d)} C_2 \left(C_7^* - 0.013\, C_8^*\right)\right]\Big\}. \tag{5}$$

The rather large coefficient in the second term has led to the observation that models with enhanced chromomagnetic dipole operators could give rise to significant changes in the rate asymmetries, compared to those of the SM [9].

The Wilson coefficients in Eq. (5) are determined using the usual Renormalization Group Evolution (RGE) procedure [11] and are to be evaluated at the b quark mass scale. The results at leading order are [12]

$$C_2(m_b) = \sum_{i=1}^{8} k_{2i} \tilde{\eta}^{a_i} \tag{6}$$

$$C_7(m_b) = \tilde{\eta}^{16/23} C_7(m_W) + \frac{8}{3}\left(\tilde{\eta}^{14/23} - \tilde{\eta}^{16/23}\right) C_8(m_W) + C_2(m_W) \sum_{i=1}^{8} h_i \tilde{\eta}^{a_i} \tag{7}$$

$$C_8(m_b) = \tilde{\eta}^{14/23} C_8(m_W) + C_2(m_W) \sum_{i=1}^{8} \overline{h}_i \tilde{\eta}^{a_i}, \tag{8}$$

where $\tilde{\eta} \equiv \alpha_s(m_W)/\alpha_s(m_b)$. The coefficients k_{2i}, h_i and $\overline{h}_i$ are tabulated in Ref. [11]. The SM expressions for the Wilson coefficients are given by

$$C_2^{\mathrm{SM}}(m_W) = 1 \tag{9}$$

$$C_7^{\mathrm{SM}}(m_W) = -\frac{1}{2} A(x_t) \tag{10}$$

$$C_8^{\mathrm{SM}}(m_W) = -\frac{1}{2} D(x_t), \tag{11}$$

where $x_t \equiv m_t^2/m_W^2$ and where A and D are the well-known "Inami-Lim" functions [13]:

$$A(x) = x\left[\frac{8x^2+5x-7}{12(x-1)^3} - \frac{(3x^2-2x)\ln x}{2(x-1)^4}\right] \tag{12}$$

$$D(x) = x\left[\frac{x^2-5x-2}{4(x-1)^3} + \frac{3x\ln x}{2(x-1)^4}\right]. \tag{13}$$

Deviations from the SM may be incorporated into the Wilson coefficients at the W mass scale and can then be run down to the b mass scale using the RGE equations given in Eqs. (6)-(8). This procedure yields the following simple expressions for $C_7(m_b)$ and $C_8(m_b)$ [9],

$$C_7(m_b) \simeq -0.31 + 0.67\, C_7^{\mathrm{new}}(m_W) + 0.09\, C_8^{\mathrm{new}}(m_W) \tag{14}$$

$$C_8(m_b) \simeq -0.15 + 0.70\, C_8^{\mathrm{new}}(m_W), \tag{15}$$

where we have used $\tilde{\eta} \simeq 0.56$ (corresponding to $\alpha_s(m_Z) = 0.118$) and where the Wilson coefficients at the W mass scale are given by

$$C_7(m_W) = C_7^{\rm SM}(m_W) + C_7^{\rm new}(m_W) \tag{16}$$
$$C_8(m_W) = C_8^{\rm SM}(m_W) + C_8^{\rm new}(m_W). \tag{17}$$

Inserting Eqs. (14) and (15) into Eq. (5) yields the following general expression for the CP asymmetry

$$A_{CP}^{b\to s(d)\gamma} \simeq \frac{10^{-2}}{|C_7(m_b)|^2}\Big\{-1.82\times {\rm Im}\,[C_7^{\rm new}] + 1.72\times {\rm Im}\,[C_8^{\rm new}] - 4.46\times {\rm Im}\,[C_8^{\rm new}C_7^{\rm new*}]$$
$$+3.21\times {\rm Im}\left[\epsilon_{s(d)}\,(1 - 2.18\,C_7^{\rm new*} - 0.26\,C_8^{\rm new*})\right]\Big\}. \tag{18}$$

Note that if $C_7^{\rm new}$ and $C_8^{\rm new}$ are approximately equal in a particular scenario, then the third term in the above expression is close to zero, and the first two terms nearly cancel one another. The main contribution to the PRA in that case is the last term. Such a scenario yields a rather small asymmetry for $b \to s\gamma$ (since the asymmetry is essentially proportional to ϵ_s), but possibly a sizable asymmetry for $b \to d\gamma$. As we shall see below, $C_7^{\rm new} \approx C_8^{\rm new}$ in multi-Higgs doublet models, so that $b \to s\gamma$ generically has a small rate asymmetry in such models.

Setting both $C_7^{\rm new}(m_W)$ and $C_8^{\rm new}(m_W)$ to zero in the above expression yields the SM predictions for the CP-violating rate asymmetries in $b \to s\gamma$ and $b \to d\gamma$,

$$A_{CP}^{b\to s(d)\gamma} \simeq 0.334\times {\rm Im}\left[\epsilon_{s(d)}\right], \tag{19}$$

or, in terms of the angles of the familiar unitarity triangle [14],

$$A_{CP}^{b\to s\gamma} \simeq 0.334\times\lambda^2\,\frac{\sin\beta_{CKM}\sin\gamma}{\sin\alpha}\,, \qquad A_{CP}^{b\to d\gamma} \simeq -0.334\times\frac{\sin\alpha\sin\beta_{CKM}}{\sin\gamma}\,. \tag{20}$$

Substituting the approximate expressions for ϵ_s and ϵ_d from Eqs. (3) and (4) and using the "best-fit" values $(\rho,\eta) = (0.20, 0.37)$ [15], we find

$$A_{CP}^{b\to s\gamma}\Big|_{SM} = 0.6\%\,, \qquad A_{CP}^{b\to d\gamma}\Big|_{SM} = -16\%\,,$$

in agreement with the estimates of previous authors [9]. The rate asymmetry for $b \to s\gamma$ is potentially a sensitive probe of non-standard physics, since its value within the SM is so small. Finding an experimental value larger than a few percent would be a strong indication of new physics. For $b \to d\gamma$, the rate asymmetry is already large within the SM; in this case, contributions due to non-standard physics might be more difficult to disentangle from the SM contribution unless they lead to an appreciable change in the PRA.

III. MULTI-HIGGS DOUBLET MODELS

One of the simplest ways to extend the SM is to expand its Higgs sector by adding extra Higgs doublets. Despite their apparent simplicity, Multi-Higgs doublet models can

have rich phenomenological consequences. Of particular interest within the context of the present work are those models that give rise to new sources of CP violation. If one imposes Natural Flavour Conservation (NFC) [16], CP violation in the charged Higgs sector does not appear until two extra Higgs doublets have been added. The Three-Higgs Doublet Model (3HDM) with NFC, incorporating spontaneous and/or explicit CP violation, has been studied extensively over the last several decades [17–21] and in many instances it leads to large CP-violating effects. Another option is to relax the requirement of NFC. In this case, CP violation appears with only one extra Higgs doublet. The so-called "Type-III" Two-Higgs doublet models can lead to interesting phenomenological consequences [22]. One variant on this class of models – the "Top-Two-Higgs Doublet Model" (T2HDM) – gives special status to the top quark [23,24]. The T2HDM has couplings unlike most other Higgs models and can produce significant effects on CP-odd observables in decays such as $B \to \psi K_S$ and $B^\pm \to \psi K^\pm$ and in D-$\overline{D}$ mixing [23–25].

Bearing in mind the above comments, it would seem natural to assume that Multi-Higgs doublet models could give rise to significant effects in the rate asymmetries for radiative b decays. This intuitive guess is correct for $b \to d\gamma$, but is *not* correct for $b \to s\gamma$. Small values for $A_{CP}^{b\to s\gamma}$ were reported in previous studies [7–10], but the reason for the smallness of the asymmetry was not elucidated. In the following we show that the rate asymmetry for $b \to s\gamma$ is typically less than a few percent in Multi-Higgs doublet models. The analogous asymmetry for $b \to d\gamma$ can nevertheless be strongly affected by the presence of extra Higgs doublets. Our general arguments will be supported by model calculations in the 3HDM and T2HDM.

The rate asymmetry for $b \to s\gamma$ is small in Higgs models because $C_8^{\rm new}(m_W)/C_7^{\rm new}(m_W) \sim 1$ in these models. As noted in the discussion following Eq. (18), this approximate equality leads to a strong suppression of the rate asymmetry. If we only consider contributions to the rate asymmetry arising from diagrams containing a charged Higgs and a top quark in the loop [26], the "new physics" corrections to C_7 and C_8 have the following general form

$$C_7^{\rm new}(m_W) = f_A A(y_t) + f_B B(y_t) \tag{21}$$

$$C_8^{\rm new}(m_W) = f_A D(y_t) + f_B E(y_t), \tag{22}$$

where $y_t \equiv m_t^2/m_H^2$, and $A(y)$ and $D(y)$ are the Inami-Lim functions introduced above. The functions $B(y)$ and $E(y)$ are given by

$$B(y) = y\left[\frac{5y-3}{12(y-1)^2} - \frac{(3y-2)\ln y}{6(y-1)^3}\right] \tag{23}$$

$$E(y) = y\left[\frac{y-3}{4(y-1)^2} + \frac{\ln y}{2(y-1)^3}\right] . \tag{24}$$

Figure 1(a) shows the various Inami-Lim functions, plotted as functions of the dimensionless variable y_t, while Fig. 1(b) shows plots of the ratios D/A and E/B. As is evident from these plots, D/A and E/B are both of order unity for Higgs masses above 100 GeV. As a result, $C_8^{\rm new}/C_7^{\rm new}$ is of order unity and the CP asymmetry for $b \to s\gamma$ is expected to be rather small. Note that the deviation from unity is slightly larger for D/A than for B/E when $m_H \sim m_t$. Thus, slightly larger asymmetries may be expected in scenarios where $f_A \gg f_B$. (See the footnote and discussion following Eq. (29).)

Let us quantify the above argument by parametrizing the deviation of $C_8^{\rm new}/C_7^{\rm new}$ from unity in terms of a complex quantity ζ. Defining

$$C_8^{\rm new}(m_W) \equiv (1+\zeta) C_7^{\rm new}(m_W) \; , \tag{25}$$

we have

$$A_{CP}^{b\to s(d)\gamma} \simeq \frac{10^{-2}}{|C_7(m_b)|^2}\Big\{ -0.10\ {\rm Im}\,[C_7^{\rm new}] + 1.72\ {\rm Im}\,[\zeta C_7^{\rm new}] - 4.46\,|C_7^{\rm new}|^2\ {\rm Im}\,[\zeta] \\ +3.21\ {\rm Im}\left[\epsilon_{s(d)}\,(1 - 2.44\ C_7^{\rm new*} - 0.26\ \zeta^* C_7^{\rm new*})\right]\Big\}. \tag{26}$$

Each of the first three terms in the above expression is small, either because it is suppressed by ζ or, in the case of the first term, because it has suffered an accidental cancellation. Since ϵ_s is itself quite small, the asymmetry for $b \to s\gamma$ will never be much larger than several percent. The present analysis is quite general and predicts that the CP asymmetry in $b \to s\gamma$ will be quite small in Higgs models. This result is independent of whether or not the corrections to the Wilson coefficients have complex phases. The situation for $b \to d\gamma$ is quite different. While it is still true that the first three terms in Eq. (26) make only a small contribution to the asymmetry, the last term now contains ϵ_d, which is relatively large and can have a significant effect on the asymmetry.

A. Three-Higgs doublet model with NFC

We now consider the 3HDM with explicit CP violation, since the 3HDM with spontaneous CP violation alone is disfavoured by data [18,21]. The charged-Higgs Yukawa couplings for this model may be written as [17]

$$L_{H^+} = (2\sqrt{2}G_F)^{\frac{1}{2}} H^+ (X\overline{U}_L V M_D D_R + Y\overline{U}_R M_U V D_L + Z\overline{N}_L M_E E_R) + {\rm H.c.} \tag{27}$$

where X, Y, and Z are complex parameters [27]. Note that the substitution $X, Z \to \tan\beta$ and $Y \to \cot\beta$ yields the Yukawa interactions of the Type-II 2HDM. The Wilson coefficients at the m_W scale are given by

$$C_7(m_W) = -\frac{1}{2}A(x_t) - XY^* B(y_t) - \frac{1}{6}|Y|^2 A(y_t) \\ C_8(m_W) = -\frac{1}{2}D(x_t) - XY^* E(y_t) - \frac{1}{6}|Y|^2 D(y_t) \; . \tag{28}$$

Thus

$$f_A = -\frac{1}{6}|Y|^2 \\ f_B = -XY^* \\ \zeta = \frac{XY^*[E(y_t) - B(y_t)] + \frac{1}{6}|Y|^2[D(y_t) - A(y_t)]}{XY^* B(y_t) + \frac{1}{6}|Y|^2 A(y_t)} \; . \tag{29}$$

In the numerical work that follows, $|\zeta|$ is typically found to be less than 0.20, so Eq. (26) yields a small asymmetry for $b \to s\gamma$, as noted above [28].

The parameter space for this 3HDM depends on four independent quantities, which may be taken to be $|X|$, $|Y|$, $\arg(XY^*)$ and m_H. The phase of Y may be absorbed into the definition of X without affecting any observable in $b \to s(d)\gamma$. We thus take Y to be real and non-negative and write X as

$$X = X_R + iX_I, \tag{30}$$

where X_R and X_I are the real and imaginary parts of X. Possible experimental constraints on X and Y come from neutral kaon decays, the neutron electric dipole moment, B-$\overline{B}$ mixing and the (CP-averaged) branching ratio for $b \to s\gamma$ [20,21,18,29]. Another constraint may be obtained by requiring the Higgs sector of the theory to be perturbative [30]. Most of these considerations lead to fairly mild constraints on the parameter space of the 3HDM. Perturbativity requires $|X| \lesssim 130$ [30], while B-$\overline{B}$ mixing requires $|Y| \lesssim 1$ for $m_H \sim 200$ GeV. The neutron electric dipole moment places a very weak constraint on $\mathrm{Im}(XY^*)$ [31,32]. A much stronger bound may be obtained from the branching ratio for $b \to s\gamma$, which yields, for example, $\mathrm{Im}(XY^*) \lesssim 3.5$ for $m_H = 200$ GeV (see Eq. (37) below, or Fig. 3). ϵ_K may also be used to constrain the parameter space of this model. If ρ and η take their SM central values, the constraint on Y is similar to that coming from B-$\overline{B}$ mixing. Long distance effects due to charged Higgs exchange may also be important for ϵ_K [18,33]. Given the theoretical uncertainties associated with long-distance calculations, we ignore such effects in our analysis.

The strongest bounds on X and Y come from the (CP-averaged) branching ratio for $b \to s\gamma$. In order to minimize uncertainties due to the mass of the bottom quark, it is common to define the ratio

$$R = \frac{\Gamma(b \to s\gamma)}{\Gamma(b \to ce\nu)}. \tag{31}$$

Calculation of R at leading order gives [34]

$$R \simeq 0.0231 \times |C_7(m_b)|^2, \tag{32}$$

where $C_7(m_b)$ is given in Eq. (14). The region allowed by the $b \to s\gamma$ branching ratio is bounded by two concentric circles in the complex X-plane for given values of Y and m_H. This may be seen by writing

$$C_7(m_b) = -c - Xd, \tag{33}$$

where c and d depend only on Y and m_H:

$$c = 0.31 + \frac{1}{6}\left[0.67A(y_t) + 0.09D(y_t)\right]|Y|^2 \tag{34}$$

$$d = \left[0.67B(y_t) + 0.09E(y_t)\right]Y. \tag{35}$$

The constraint due to the measured rate for $b \to s\gamma$ then takes the general form

$$R^{\min} \leq 0.0231 \times d^2 \left[\left(X_R + \frac{c}{d}\right)^2 + X_I^2\right] \leq R^{\max}; \tag{36}$$

that is, the allowed region is bounded by two concentric circles in the complex X-plane. $R^{\rm max}$ and $R^{\rm min}$ depend on the experimental value for the ratio R as well as on various experimental and theoretical uncertainties. The above expression may be used to find an upper bound on $|{\rm Im}(XY^*)|$. In terms of the geometrical picture presented above, the upper bound occurs at the "top" and "bottom" of the outer circle, yielding

$$|{\rm Im}(XY^*)| \leq \frac{1}{0.67B(y_t) + 0.09E(y_t)} \sqrt{\frac{R^{\rm max}}{0.0231}} \, . \tag{37}$$

A search of the parameter space for this 3HDM yields results consistent with the general arguments given for Higgs models at the beginning of Sec. III. The rate asymmetry for $b \to s\gamma$ is found to be smaller than three or four percent, while that for $b \to d\gamma$ can vary between $\pm 20\%$. Figures 2 and 3 show plots that are representative of the results obtained. In each figure, contours of constant asymmetry for $b \to s(d)\gamma$ are shown in the (X_R, X_I) plane for fixed values of Y and m_H. Labels for the various contours are given as percentages. The size of the ring-shaped allowed region is determined by the maximum and minimum values allowed for the ratio R. The current experimental value for this ratio may be determined by using the weighted average of the CLEO [1] and ALEPH [2] values for the $b \to s\gamma$ branching ratio, $\mathcal{B}(B \to X_s\gamma)|_{\rm ave} \simeq (3.14 \pm 0.48) \times 10^{-4}$, as well as the branching ratio for $b \to ce\nu$, $\mathcal{B}(B \to X_c e\nu) \simeq 0.104 \pm 0.009$ [35]. This procedure yields the value $R = (3.02 \pm 0.53) \times 10^{-3}$. In addition to the experimental uncertainty for this ratio, there is another theoretical uncertainty. Since we are using LO expressions for the Wilson coefficients, we estimate the magnitude of this uncertainty to be $\delta R^{\rm theory} = 0.7 \times 10^{-3}$. Combining the experimental and theoretical uncertainties in quadrature and doubling the result to get a "2σ" uncertainty, we obtain $R^{\rm min} = 0.0013$ and $R^{\rm max} = 0.0048$. These are the values used in the plots.

Figure 2 compares the asymmetries obtained for two different values of the Higgs mass with Y held constant, while Fig. 3 keeps m_H constant and shows the effect of changing Y. While the size of the allowed region exhibits a strong dependence on the values chosen for Y and m_H (note the changes in the horizontal and vertical scales in the plots), the contours themselves look very similar from plot to plot. This is particularly true in the case of $b \to d\gamma$, whose asymmetry contours appear to be exact replicas of one another once an appropriate scaling and shifting has been performed in the (X_R, X_I) plane. In order to understand the scaling behaviour of $A_{CP}^{b\to d\gamma}$, it is easiest to return to one of the original rate asymmetry expressions, Eq. (5). The first three terms in Eq. (5) are identical for $b \to s\gamma$ and $b \to d\gamma$ in this model. According to the discussion following Eq. (26), these terms combine to give a contribution to the asymmetry of at most a few percent. A good approximation for $b \to d\gamma$ is thus obtained by neglecting these terms altogether (as well as the small contribution proportional to $\epsilon_d C_2 C_8^*$) and writing

$$A_{CP}^{b\to d\gamma} \simeq \frac{-9.40 \times 10^{-2}}{|C_7(m_b)|^2} \times {\rm Im}\left[\epsilon_d C_2 C_7^*\right] . \tag{38}$$

Changes in Y or m_H lead to changes in the functions c and d defined in Eqs. (34) and (35). It is always possible to perform a linear transformation on X_R and X_I that compensates for this change and leaves $C_7(m_b)$ invariant. Since both the above approximate expression

for $A_{CP}^{b\to d\gamma}$ and the expression for the rate, Eq. (32), depend only on $C_7(m_b)$, they too are invariant under this transformation [36]. The variations in the contours for $b \to s\gamma$ may be attributed to the fact that $C_8(m_b)$ – which has a larger effect on $b \to s\gamma$ – is not invariant under the transformation.

Figure 4 shows a few representative correlation plots demonstrating the relationship between the asymmetries for $b \to s\gamma$ and $b \to d\gamma$. It also shows the relationship between the asymmetry and branching ratio for $b \to d\gamma$. The branching ratios in these plots have been normalized to the theoretical expression for $\mathcal{B}(b \to s\gamma)$ within the SM. The ratio of branching ratios has the simple form

$$\frac{\mathcal{B}_{\rm 3HDM}(b \to d\gamma)}{\mathcal{B}_{\rm SM}(b \to s\gamma)} = \left|\frac{V_{td}}{V_{ts}}\right|^2 \left|\frac{C_7(m_b)|_{\rm 3HDM}}{C_7(m_b)|_{\rm SM}}\right|^2 . \tag{39}$$

The points for these plots are taken to be uniformly distributed on square grids inside the respective allowed regions in the complex X-plane. This method of choosing points leads to the observed "textures" in these plots.

B. Type-III Two-Higgs Doublet Models

In Two-Higgs Doublet Models with natural flavour conservation [16] (as in types I and II [37]), there exist no new CP-violating phases in the charged-Higgs Yukawa couplings beyond that of the Cabibbo-Kobayashi-Maskawa (CKM) [38] matrix. Consequently, the charged Higgs contribution to the $b \to s\gamma$ rate asymmetry is both CKM- and QCD-suppressed (the latter by a factor α_s/π) and the asymmetry is small, as in the SM. The $b \to d\gamma$ rate asymmetry is also similar to its SM value of approximately -16%. In Type III 2HDM's [22], where no *adhoc* discrete symmetry is imposed, one generally expects new CP-violating phases in the Yukawa couplings (as well as flavour-changing neutral Higgs interactions). As a result, the CKM and GIM suppressions present in the SM for $b \to s\gamma$ are in general no longer operative, and a potentially large partial rate asymmetry in $b \to s\gamma$ seems possible. This expectation is invalid due to the accidental cancellation mechanism discussed above.

As a concrete example of a Type-III 2HDM, we consider the 2HDM for the top quark (T2HDM) [23,24]. This model is designed to accommodate the heaviness of the top quark by coupling it to a scalar-doublet with a large VEV. The other five quarks are coupled to the other scalar-doublet, whose VEV is much smaller. As a result, $\tan\beta$ is naturally large in this model. A distinctive feature of the T2HDM is its $\tan\beta$-enhanced charm quark Yukawa coupling, with the consequence that the charged Higgs sector can significantly affect the neutral kaon system and the $b \to s\gamma$ rate.

Although there are two new CP phases in the T2HDM from the unitary rotation of the right-handed up-type quarks, only one of them contributes to radiative b decays. This is the phase δ of the complex parameter $\xi = |\xi|e^{-i\delta}$, measuring the c_R-t_R mixing [24]. As was done before, we take $|\xi| = 1$ throughout this paper. In contrast with the 3HDM, the virtual charm quark contribution in the T2HDM can occasionally be of the same magnitude as that of the top quark. The Wilson coefficient for $b \to q\gamma$ ($q = s, d$) is given by [24]

$$C_7^{\rm new}(m_W) = \sum_{i=c,t} \kappa^{iq} \left[-\tan^2\beta + \frac{1}{m_i V_{iq}^*} \left(\Sigma^T V^*\right)_{iq} \left(\tan^2\beta + 1\right)\right]$$

$$\times \left\{ B(y_i) + \frac{1}{6} A(y_i) \left[-1 + \frac{1}{m_i V_{ib}} \left(\Sigma^\dagger V \right)_{ib} \left(\cot^2 \beta + 1 \right) \right] \right\}, \tag{40}$$

where $\kappa^{iq} = -V_{ib} V_{iq}^* / (V_{tb} V_{tq}^*)$, $y_i = (m_i/m_H)^2$, and V denotes the CKM matrix. The definition of the matrix Σ may be found in [24]. The expression for $C_8^{\rm new}(m_W)$ is obtained from $C_7^{\rm new}(m_W)$ by the substitutions $A(y_i) \to D(y_i)$ and $B(y_i) \to E(y_i)$.

We have studied the rate asymmetries over much of the parameter space in this model and have found the PRA for $b \to s\gamma$ to be very small, consistent with our general observations above. For $b \to d\gamma$, the PRA shows a strong dependence on the CKM phase (see Eq. (38)) but is barely affected by the new phase δ. Interestingly, the CKM phase can take a wide range of values in this model because the observed CP violation in the neutral kaon system may come partly or solely from the charged Higgs sector [24]. As a result, the PRA for $b \to d\gamma$ can be very different from the SM expectation, and can even be quite small. These features are illustrated in Figs. 5 and 6. The shaded regions in these plots indicate the "allowed" regions, while the white regions are ruled out by constraints coming from ϵ_K, Δm_K and the branching ratio for $b \to s\gamma$. The constraints coming from ϵ_K and Δm_K were discussed in detail in Ref. [24] for several scenarios and have been adopted here without change for similar scenarios. Figure 5 illustrates the case of a SM-like scenario: the Wolfenstein parameters ρ and η take their SM best fit values, and the CP asymmetry for $b \to d\gamma$ varies in the neighborhood of its SM prediction. Figure 6 shows a real-CKM scenario, where $\eta = 0$ and $\rho = 0.42$. In this case the CP asymmetry for $b \to d\gamma$ is close to zero. Note that the recent CDF measurement of the CP asymmetry in $B \to \psi K_S$ [39] disfavours a negative value for η, both within the SM and within the T2HDM [24]. We thus estimate the maximum CP asymmetry for $b \to d\gamma$ within the T2HDM to be of order $+4\%$, as indicated in Fig. 6.

It is worthwhile to compare the rate asymmetries in the 3HDM and the T2HDM. It is evident from Figs. 2-6 that the rate asymmetry for $b \to s\gamma$ is small in both models, as argued above on general grounds. In contrast, the rate asymmetry for $b \to d\gamma$ in these models can differ appreciably from its SM value, -16%, taking on values between $\pm 20\%$ in the 3HDM and between approximately -16% and $+4\%$ in the T2HDM. An important difference between the two models is that $A_{CP}^{b\to d\gamma}$ in the T2HDM is almost completely determined by the CKM phase, while the analogous asymmetry for the 3HDM exhibits a strong dependence on the charged Higgs sector CP-violating phase.

IV. SUPERSYMMETRY

Supersymmetric predictions for the $b \to s\gamma$ rate asymmetry are highly model-dependent [5,9,40–46]. Restrictive models, such as minimal supergravity, yield asymmetries of order 2% or less when the electron and neutron electric dipole moment constraints are taken into account [40]. Relaxing some of the assumptions of minimal supergravity leads to asymmetries as large as 10% [41], while allowing for non-CKM-like intergenerational squark mixing can lead to asymmetries of order 15% [42,43] or larger if the gluino mass is significantly lighter than the squark masses [9]. In this latter case, gluino-mediated diagrams become important in addition to the usual chargino- and charged Higgs-mediated diagrams. Allowing for the violation of R-parity can lead to asymmetries of order 17% [46]. A recent calculation of the $b \to d\gamma$ rate asymmetry in a fairly restrictive supersymmetric scenario yielded values in the ranges $-(5-45)\%$ and $+(2-21)\%$ [47].

The $b \to s\gamma$ rate asymmetry within supersymmetric models can be appreciably larger than that in Higgs models or in the SM. It is instructive to see how supersymmetric models evade the accidental cancellation encountered by Higgs models. In order to understand this, let us consider the chargino-squark loop contributions that must typically be added to the W and charged Higgs contributions considered thus far. These diagrams give rise to additional terms in the Wilson coefficients [48], which we denote by

$$C_7^\omega(m_W) = f_C K_1^7(y) + f_D K_2^7(y) \ , \tag{41}$$
$$C_8^\omega(m_W) = f_C K_1^8(y) + f_D K_2^8(y) \ . \tag{42}$$

Here f_C and f_D parameterize the couplings and y is the square of the ratio of the chargino and squark masses. The chargino loop for C_7 involves two new Inami-Lim functions, $K_1^7 = 6A(y) + 5D(y)$ and $K_2^7 = 6B(y) + 5E(y)$, whereas for C_8 the two functions are given by $K_1^8 = 9A(y) - 6D(y)$ and $K_2^8 = 9B(y) - 6E(y)$. Since $D/A \sim 1$ and $E/B \sim 1$, we have $K_1^8/K_1^7 \sim 3/11$ and $K_2^8/K_2^7 \sim 3/11$. As a result, $C_7^\omega(m_W)$ is generically a few times larger than $C_8^\omega(m_W)$, and there is no longer a cancellation between the first two terms of Eq. (18). Thus, a large asymmetry in supersymmetric theories is possible.

V. COMMENTS ON EXPERIMENTAL TECHNIQUES AND SENSITIVITIES

The experimental detection of the inclusive process $B \to X_d\gamma$ (i.e., $b \to d\gamma$) is very challenging. The main difficulty is that the smaller signal for $b \to d\gamma$ must be isolated from the much larger "background" of $b \to s\gamma$. This requires ensuring that the signal events for $b \to d\gamma$ do not carry net strangeness. In the following we discuss two ideas that may be used to determine the branching ratio and partial rate asymmetry for $B \to X_d\gamma$. We also compare the experimental sensitivity to the PRA's for $b \to s\gamma$ and $b \to d\gamma$.

A. Multiplicity cut

One strategy that may be helpful in determining $\mathcal{B}(B \to X_d\gamma)$ is to use a multiplicity cut so that one deals with a semi-inclusive sample consisting of a maximum of n (say 5) mesons. Using such a measurement along with the corresponding one for $B \to X_s\gamma$, one can deduce the *total* inclusive rate for $B \to X_d\gamma$ to a very good approximation via:

$$\frac{\mathcal{B}(B \to X_d\gamma)}{\mathcal{B}(B \to X_s\gamma)} \approx \frac{\Gamma(B \to \gamma + 2\pi) + \Gamma(B \to \gamma + 3\pi) + \cdots + \Gamma(B \to \gamma + n\pi)}{\Gamma(B \to \gamma + K + \pi) + \Gamma(B \to \gamma + K + 2\pi) + \cdots + \Gamma(B \to \gamma + K + (n-1)\pi)} \tag{43}$$

Note that each value of n for which a measurement is available leads to such an equation. Thus, in principle, the measurements could be repeated for different values of n to help reduce systematic uncertainties [49]. There are two key assumptions used in Eq. (43). The first is that $SU(3)$ holds; this assumption could introduce errors at the 10% level. The second assumption is that non-spectator contributions may be ignored – i.e., Eq. (43) assumes that the spectator approximation holds precisely. This latter assumption should work very well

for neutral B's. For charged B's, the annihilation graph can make a contribution of order 20% [50], so that Eq. (43) will receive somewhat larger corrections for $B^{\pm}$; nevertheless Eq. (43) provides an excellent basis for the determination of an approximate expression for $\mathcal{B}(B \to X_d\gamma)$.

B. End point study via an energy cut

Another possibility is to place a mass cut on the recoiling hadron so that $m_X < (m_\pi + m_K) \sim 635$ MeV. Correspondingly there is a minimum energy cut on the photon, e.g., $E_\gamma \gtrsim 2.60$ GeV [51]. This would ensure that the decay products result from $b \to d\gamma$ and not from $b \to s\gamma$. PRA determination from this would be quite straightforward:

$$A_{CP}^{b\to d\gamma}\Big|_{E_\gamma > E_\gamma^{\rm min}} = \frac{\mathcal{B}'(\overline{B} \to X_d\gamma) - \mathcal{B}'(B \to X_{\overline{d}}\gamma)}{\mathcal{B}'(\overline{B} \to X_d\gamma) + \mathcal{B}'(B \to X_{\overline{d}}\gamma)} \,, \tag{44}$$

where $\mathcal{B}'$ stands for the branching ratio with the energy cut on the photon.

C. PRA in $b \to d\gamma$

Since the number of B's needed for searching for a given asymmetry A_{CP} scales approximately as $(\mathcal{B}A_{CP}^2)^{-1}$, the PRA in $b \to d\gamma$ is statistically much more accessible than that in $b \to s\gamma$. The point is that, based on the SM, the PRA in $b \to d\gamma$ is expected to be 20-40 times larger than that in $b \to s\gamma$. Not only does this offset the difference in their branching ratios, it may even overcome the decrease in detection efficiency for $b \to d\gamma$.

As an illustration, suppose $\mathcal{B}(B \to X_d\gamma) \sim \mathcal{B}(B \to X_s\gamma)/20 \sim 1.5 \times 10^{-5}$. Then, to establish a 16% PRA to 3σ significance with a 20% detection efficiency and a 25% tagging efficiency, the needed number of B-$\overline{B}$ pairs is:

$$N_B^{3\sigma} \sim \frac{9}{1.5 \times 10^{-5} \times 0.2 \times 0.25 \times 0.16 \times 0.16} = 4.7 \times 10^8 \tag{45}$$

In contrast, let us take $A_{CP}^{b\to s\gamma} \simeq 0.6\%$, a detection efficiency of 70% and a 50% tagging efficiency. In this case the number of B-$\overline{B}$ pairs needed is:

$$N_B^{3\sigma} \sim \frac{9}{3.2 \times 10^{-4} \times 0.7 \times 0.50 \times 0.006 \times 0.006} = 2.2 \times 10^9 \tag{46}$$

Therefore, establishing a PRA in $b \to d\gamma$ may be less difficult than in $b \to s\gamma$.

VI. CONCLUDING REMARKS

The study of CP violation in B decays is one of the central themes at the various B-facilities. In particular, the standard model CKM paradigm of CP violation will be tested and new sources of CP violation will be searched for. In this work, we have shown that the charged Higgs loop contribution to the rate asymmetry in $b \to s\gamma$ is small in all models due to an accidental cancellation in the loop integrals. More specifically, in charged Higgs models,

$C_8^{\rm new} \sim C_7^{\rm new}$. As a result, the first two terms in Eq. (18) nearly cancel and the third term is suppressed, leading to a small asymmetry. Therefore, any experimental discovery of direct CP violation in $b \to s\gamma$ at the 10% level will be due to new sources of CP violation beyond charged Higgs, for example supersymmetry. We have also explained why chargino loops in supersymmetry do not undergo this cancellation. This is because $C_7^{\omega}(m_W)$ is generically a few times larger than $C_8^{\omega}(m_W)$. Consequently, sizeable asymmetries are possible within supersymmetry.

The direct CP asymmetry in $b \to d\gamma$ behaves quite differently from its counterpart in $b \to s\gamma$. In Multi-Higgs doublet models, the asymmetry can be large and of opposite sign relative to the SM. In the T2HDM, in particular, CP violation is mainly determined by the CKM phase, and the asymmetry can show a strong deviation from the SM prediction if the observed CP violation in the neutral kaon system has a sizable component from the charged Higgs sector. These features make the the experimental measurement of the rate asymmetry in $b \to d\gamma$ very worthwhile. Our main results are summarized in Table I along with representative results from various other models.

We have also offered some suggestions that we hope would lead to the measurement of the inclusive decay $\mathcal{B}(B \to X_d\gamma)$, and eventually even the PRA in that mode.

ACKNOWLEDGMENTS

This research was supported in part by the U.S. Department of Energy contract numbers DE-AC02-98CH10886 (BNL) and DE-FG03-96ER40969 (Oregon). K.K. is supported by an award from Research Corporation and by the SRTP at Taylor University. G.W. would like to thank the BNL theory group for its hospitality during the final stage of this work.

REFERENCES

[1] CLEO Collaboration, S. Ahmed *et al.*, CLEO CONF 99-10, hep-ex/9908022. The three uncertainties represent the statistical, systematic and model dependence uncertainties, respectively.

[2] ALEPH Collaboration, R. Barate *et al.*, Phys. Lett. B **429**, 169 (1998).

[3] K. Chetyrkin, M. Misiak and M. Münz, Phys. Lett. B **400**, 206 (1997); erratum *ibid* B **425**, 414 (1998).

[4] A. Czarnecki and W.J. Marciano, Phys. Rev. Lett. **81**, 277 (1998).

[5] A. Kagan and M. Neubert, Eur. Phys. J. **C7**, 5 (1999).

[6] J. Soares, Nucl. Phys. B **367**, 575 (1991).

[7] L. Wolfenstein and Y.L. Wu, Phys. Rev. Lett **73**, 2809 (1994); G.M. Asatrian and A. Ioannisian, Phys. Rev. D **54**, 5642 (1996).

[8] H.M. Asatrian, G.K. Egiian, and A.N. Ioannisian, Phys. Lett. B **399**, 303 (1997).

[9] A.L. Kagan and M. Neubert, Phys. Rev. D **58**, 094012 (1998).

[10] F. Borzumati and C. Greub, Phys. Rev. D **58**, 074004 (1998).

[11] G. Buchalla, A.J. Buras and M.E. Lautenbacher, Rev. Mod. Phys. **68**, 1125 (1996).

[12] Note that $C_{7,8}(m_b)$ are often denoted by $C_{7,8}^{\rm eff}(m_b)$ in the literature.

[13] T. Inami and C.S. Lim, Prog. Theor. Phys. **65**, 297 (1981).

[14] We add the subscript to β_{CKM} in order to distinguish it from $\beta \equiv \tan^{-1} v_2/v_1$.

[15] A. Ali and D. London, Eur. Phys. J. **C9**,687 (1999); F. Caravaglios, F. Parodi, P. Roudeau and A. Stocchi, hep-ph/0002171; M. Artuso, hep-ph/9911347, in the proceedings of *International Europhysics Conference on High-Energy Physics, July, 1999, Tampere, Finland.*

[16] S. Glashow and S. Weinberg, Phys. Rev. D **15**, 1958 (1977).

[17] S. Weinberg, Phys. Rev. Lett. **37**, 657 (1976); C.H. Albright, J. Smith and S.-H.H. Tye, Phys. Rev. D **21**, 711 (1980); K. Shizuya and S.-H.H. Tye, Phys. Rev. D **23**, 1613 (1981).

[18] D. Chang, X.-G. He and B.H.J. McKellar, hep-ph/9909357.

[19] D. Atwood, G. Eilam and A. Soni, Phys. Rev. Lett. **71**, 492 (1993).

[20] Y. Grossman, Nucl. Phys. B **426**, 355 (1994).

[21] Y. Grossman and Y. Nir, Phys. Lett. B **313**, 126 (1993).

[22] T.P. Cheng and M. Sher, Phys. Rev. D **35**, 3484 (1987); W.-S. Hou, Phys. Lett. B **296**, 179 (1992); M. Luke and M. Savage, Phys. Lett. B **307**, 387 (1993); L. Hall and S. Weinberg, Phys. Rev. D **48**, R979 (1993); Y. L. Wu and L. Wolfenstein, Phys. Rev. Lett. **73**, 1762 (1994), and Y. L. Wu, hep-ph/9404241; D. Atwood, L. Reina, and A. Soni, Phys. Rev. D **55**, 3156 (1997); Phys. Rev. D **53**, 1199 (1996); D. Bowser-Chao, K. Cheung, and W.-Y. Keung, Phys. Rev. D **59**, 115006 (1999).

[23] A. Das and C. Kao, Phys. Lett. B **372**, 106 (1996).

[24] K. Kiers, A. Soni, and G.-H. Wu, Phys. Rev. D **59**, 096001 (1999); G.-H. Wu and A. Soni, *ibid.* **62**, 056005 (2000), hep-ph/9911419.

[25] Y.-F. Zhou and Y.-L. Wu, Mod. Phys. Lett. **A 15**, 185 (2000).

[26] In models that do not enforce NFC there can also be flavour-changing neutral Higgs interactions. Also, in the T2HDM (to be discussed below), there are contributions from the charm quark that should be taken into account.

[27] We only consider effects due to the lighter of the two physical charged Higgs.

[28] If $X \approx 0$ the $|Y|^2$ terms in Eq. (29) dominate and $\zeta \simeq D/A - 1$, which can be relatively large for small Higgs masses (see Fig. 1(b)). For $m_H = 150$ GeV and $X = 0$, for example, $|\zeta| \simeq 0.42$. The asymmetry is still very small, however, due to the smallness of Y and to the factor of "1/6" appearing in Eq. (28). Moderate values of ζ can also occur if the XY^* terms dominate and m_H is very large; however, large Higgs masses tend to suppress the nonstandard contributions to $A_{CP}^{b\to s\gamma}$.
[29] J.L. Hewett, hep-ph/9406302, in *Proceedings of the SLAC Summer Inst. on Particle Physics: Spin Structure in High Energy Processes, Stanford, CA (1993).*
[30] V. Barger, J.L. Hewett and R.J.N. Phillips, Phys. Rev. **D 41**, 3421 (1990).
[31] P. Krawczyk and S. Pokorski, Nucl. Phys. B **364**, 10 (1991); Y. Nir, in *Proceedings of the SLAC Summer Inst. on Particle Physics: The Third Family and the Physics of Flavor*, page 81, ed. L. Vassilian (SLAC-Report-412, 1993)
[32] BABAR Collaboration, *The BABAR Physics Book: Physics at an Asymmetric B Factory,* P.F. Harrison and H.R. Quinn, eds., Report No. SLAC-R-504.
[33] J. Donoghue and B. Holstein, Phys. Rev. D **32**, 1152 (1985); H.-Y Cheng, Phys. Rev. D **34**, 1397 (1986).
[34] See Refs. [11] and [4]. We use $\alpha_{\rm em}$, as suggested in Ref. [4].
[35] Particle Data Group, C. Caso *et al.*, Eur. Phys. J. **C3**, 1 (1998).
[36] It is straightforward to show that the transformation on X_R and X_I leads to a shift and rescaling that leaves the "shapes" of the contours and that of the circular allowed region invariant with respect to each other.
[37] For a review, see J. Gunion *et al.*, *The Higgs Hunter's Guide*, Addison-Wesley, Redmond City, CA 94065-1522, 1990.
[38] M. Kobayashi and T. Maskawa, Prog. Theor. Phys. **49**, 652 (1973).
[39] CDF Collaboration, T. Affolder *et al.*, Phys. Rev. D **61**, 072005 (2000).
[40] T. Goto ,Y.-Y. Keum, T. Nihei, Y. Okada and Y. Shimizu, Phys. Lett. B **460**, 333 (1999).
[41] M. Aoki, G.-C. Cho and N. Oshimo, Phys. Rev. D **60**, 035004 (1999); Nucl. Phys. B **554**, 50 (1999).
[42] C.-K. Chua, X.-G. He and W.-S. Hou, Phys. Rev. D **60**, 014003 (1999).
[43] Y.G. Kim, P. Ko and J.S. Lee, Nucl. Phys. B **544**, 64 (1999).
[44] S. Baek and P. Ko, Phys. Rev. Lett. **83**, 488 (1999).
[45] L. Giusti, A. Romanino and A. Strumia, Nucl. Phys. B **550**, 3 (1999).
[46] E.J. Chun, K. Hwang and J.S. Lee, hep-ph/0005013.
[47] H.H. Asatryan and H.M. Asatrian, Phys. Lett. B **460**, 148 (1999).
[48] See, for example, Ref. [41].
[49] In using Eq. (43), contributions from resonance channels (such as $B \to K^*\gamma$, $B \to \rho\gamma$,...) can easily be excluded or included, by using the final states into which the resonances decay, as long as the numerator and denominator are treated in the same way.
[50] D. Atwood, B. Blok and A. Soni, Int. J. Mod. Phys. **A 11**, 3743 (1996); G. Eilam, A. Ioannissian and R. R. Mendel, Z. Phys. C **71**, 95 (1996); A. Ali and V. M. Braun, Phys. Lett. B **359**, 223 (1995); A. Khodjamirian, R. Ruckl, G. Stoll and D. Wyler, Phys. Lett. B **358**, 129 (1995); B. Grinstein and D. Pirjol, hep-ph/0002216.
[51] Once again from a measurement of the partial width in such a kinematic window, we

can deduce the branching ratio by appealing to $SU(3)$: $\mathcal{B}(B \to X_d\gamma)/\mathcal{B}(B \to X_s\gamma) \simeq \mathcal{B}'(B \to X_d\gamma)/\mathcal{B}'(B \to X_s\gamma)$, where the photon energy cuts for the two decay modes have the same fraction of their respective available energies.

[52] SuperKamiokande Collaboration, Y. Fukuda *et al.*, Phys. Rev. Lett. **82**, 2644 (1999).

TABLES

Model	$A_{CP}^{b\to s\gamma}$ (%)	$A_{CP}^{b\to d\gamma}$ (%)
SM	0.6	-16
2HDM (Model II)	~ 0.6	~ -16
3HDM	-3 to $+3$	-20 to $+20$
T2HDM	~ 0 to $+0.6$	~ -16 to $+4$
Supergravity [40,41,47]	~ -10 to $+10$	$-(5-45)$ and $+(2-21)$
SUSY with squark mixing [42,43,9]	~ -15 to $+15$	
SUSY with R-parity violation [46]	~ -17 to $+17$	

TABLE I. CP asymmetries in various models. Quoted ranges are approximate; see the text for details. The blank entries represent quantities that have not, to our knowledge, been considered in the literature. The rate asymmetry for $b \to s\gamma$ from SUSY with squark mixing could be larger than the quoted $\pm 15\%$ if the gluino mass is significantly lighter than the squark masses [9]. Note that the range quoted for the R-parity violating case assumes $m_{\nu_\tau} \sim 10$ keV. The asymmetry is negligible if $m_{\nu_\tau} \ll 10$ keV, as is indicated by the SuperKamiokande atmospheric neutrino oscillation data [52].

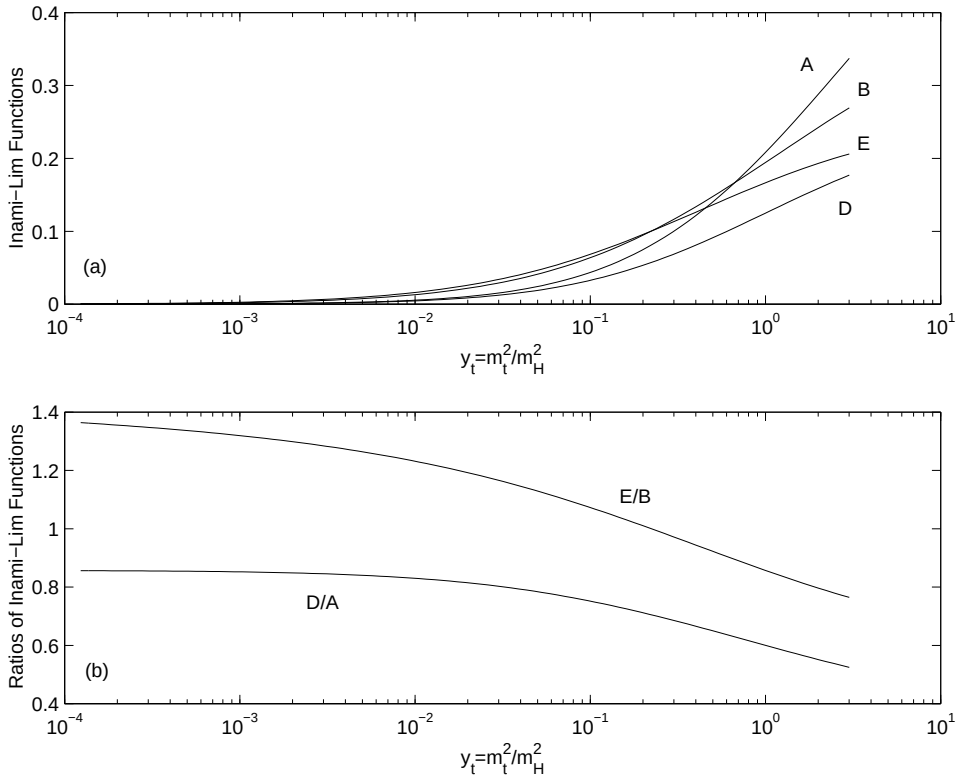

FIG. 1. (a) The Inami-Lim functions as defined in the text. (b) Ratios of the Inami-Lim functions.

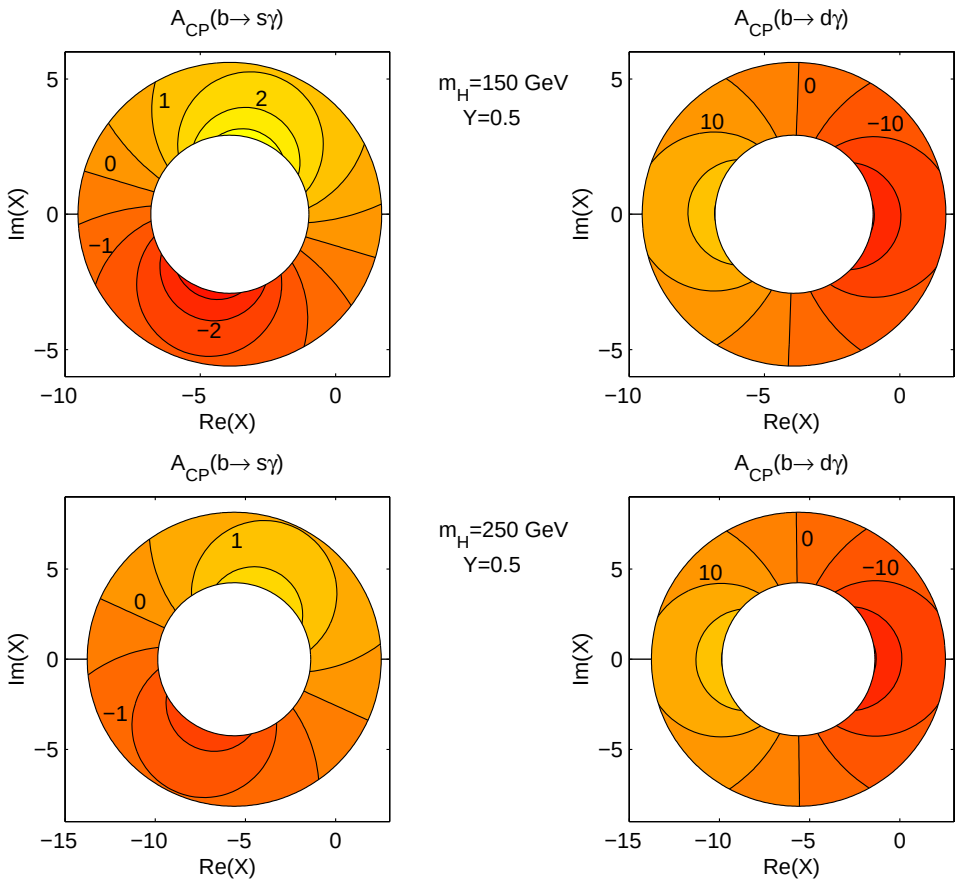

FIG. 2. Contour plots of partial rate asymmetries in the decays $b \to s\gamma$ and $b \to d\gamma$ in the 3HDM with $\rho = 0.20$ and $\eta = 0.37$. The shaded ring-like regions are experimentally allowed. The contour lines show the CP asymmetries as percentages.

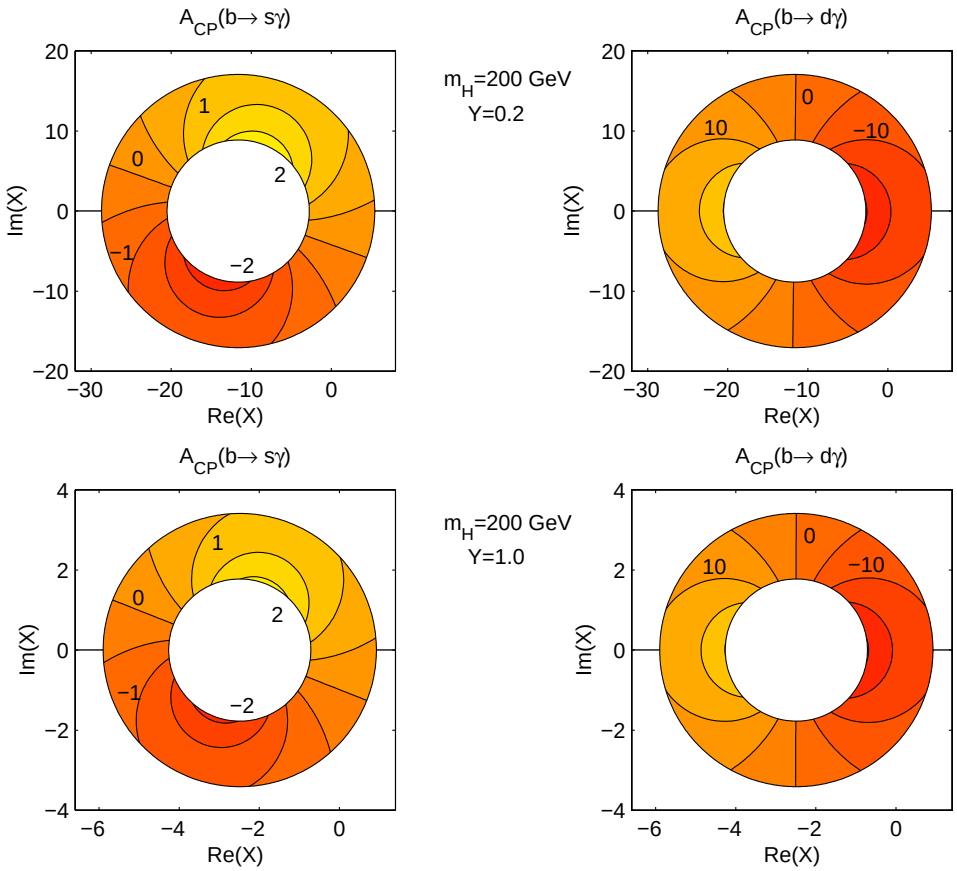

FIG. 3. Same as Fig. 2, but with different values for m_H and Y.

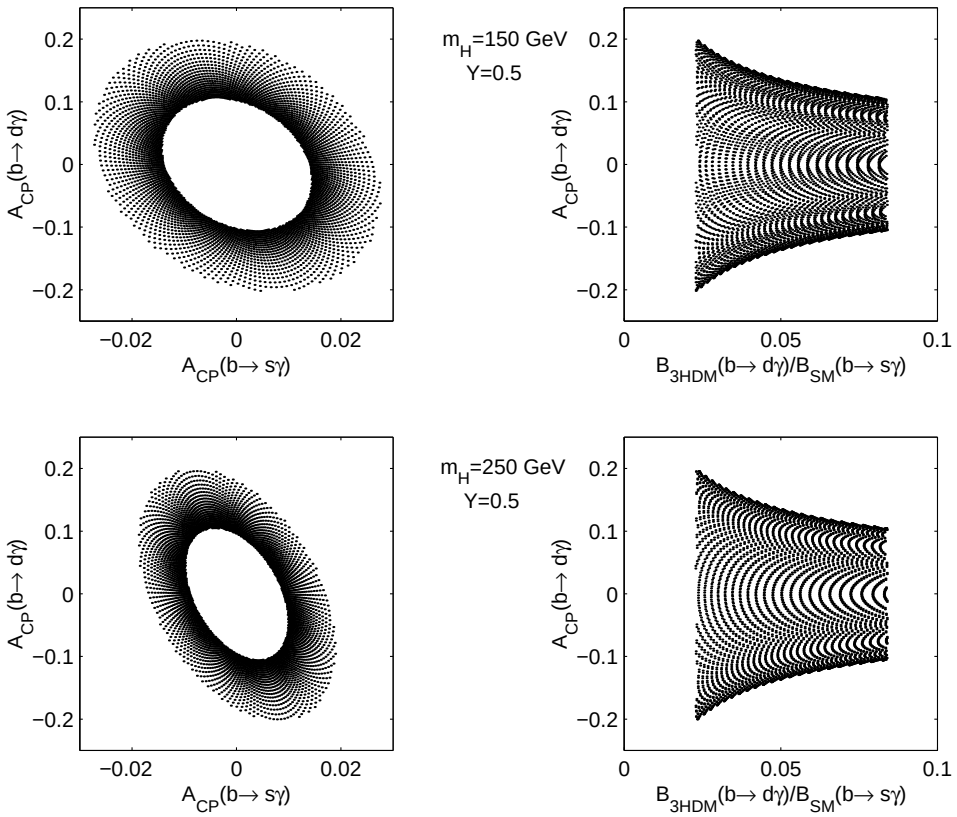

FIG. 4. Correlation between the rate asymmetries of $b \to s\gamma$ and $b \to d\gamma$ in the 3HDM. Also shown are the ranges of the ratio of branching ratios for the radiative decays.

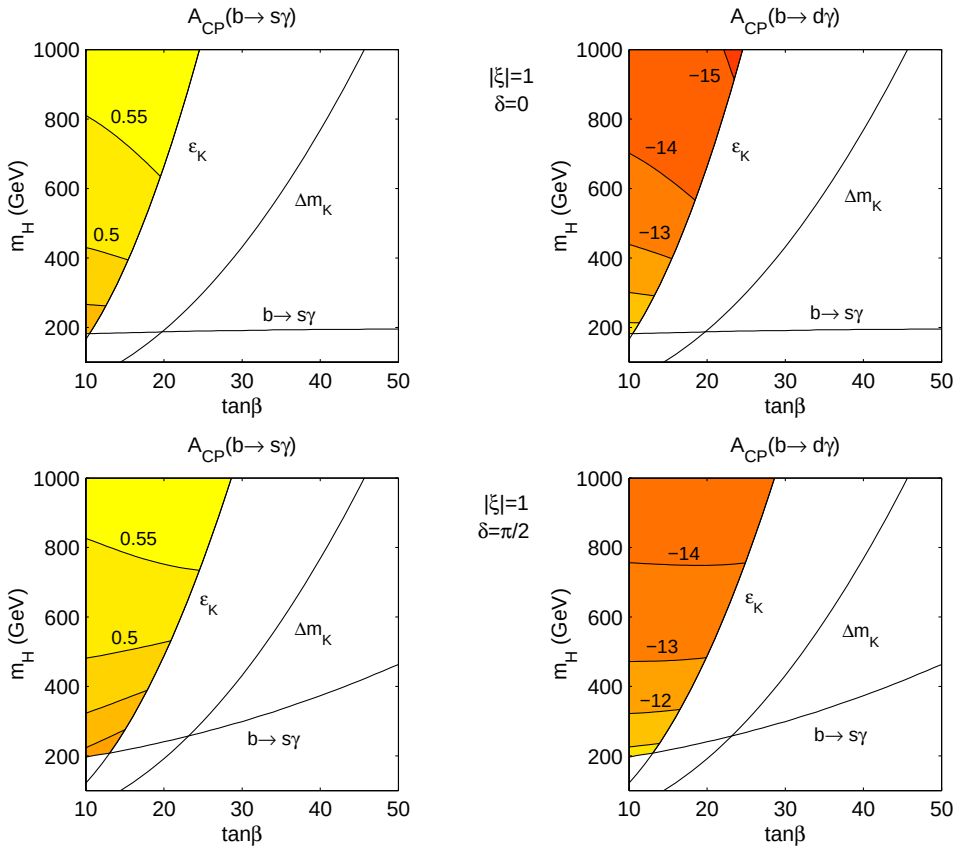

FIG. 5. Contour plots of PRA's in $b \to s\gamma$ and $b \to d\gamma$ in the T2HDM – SM-like scenario: ρ and η take their SM best fit values ($\rho = 0.20$ and $\eta = 0.37$). The experimentally allowed regions are shaded, and the contours show the asymmetries as percentages.

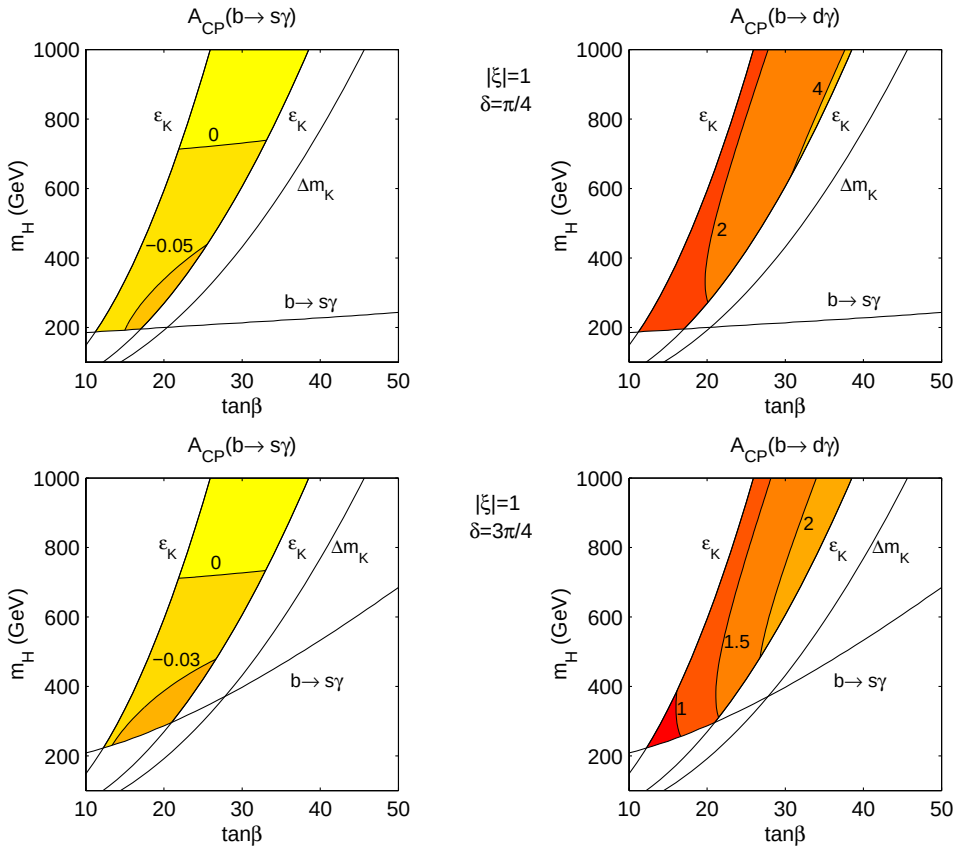

FIG. 6. Similar to Fig. 5, but with a real CKM matrix.